AGU PUBLICATIONS

JGR

Journal of Geophysical Research: Atmospheres

RESEARCH ARTICLE
10.1002/2017JD026590

Key Points:
- Suomi NPP VIIRS long-wave infrared bands have been working well, except for $a \sim 0.1$ K bias found during blackbody unsteady states
- Our analysis shows that this anomaly is traced to a key assumption of calibration curve shape in the algorithm theoretical basis
- A diagnostic method and correction algorithm is developed and tested to resolve this bias

Correspondence to:
C. Cao,
changyong.cao@noaa.gov

Citation:
Cao, C., W. Wang, S. Blonski, and B. Zhang (2017), Radiometric traceability diagnosis and bias correction for the Suomi NPP VIIRS long-wave infrared channels during blackbody unsteady states, *J. Geophys. Res. Atmos.*, *122*, 5285–5297, doi:10.1002/2017JD026590.

Received 2 FEB 2017
Accepted 7 MAY 2017
Accepted article online 15 MAY 2017
Published online 27 MAY 2017

Radiometric traceability diagnosis and bias correction for the Suomi NPP VIIRS long-wave infrared channels during blackbody unsteady states

Changyong Cao[1], Wenhui Wang[2], Slawomir Blonski[2], and Bin Zhang[2,3]

[1]NOAA/Center for Satellite Applications and Research, College Park, Maryland, USA, [2]ERT Inc., Laurel, Maryland, USA, [3]CICS, University of Maryland, College Park, Maryland, USA

Abstract The Suomi National Polar-orbiting Partnership Program (NPP) Visible Infrared Imaging Radiometer Suite (VIIRS) Thermal Emissive Bands (TEBs) have been performing well since the data became available on 20 January 2012, and the Sensor Data Record data reached validated maturity on 18 March 2014. While overall the validation has shown that these channels have an estimated absolute uncertainty on the order of 0.1 K based on extensive comparisons, there is a remaining issue that persisted over the years. A calibration bias on the order of 0.1 K is introduced in channels such as M15 during the quarterly blackbody temperature warm-up/cooldown, and the bias is further amplified by the sea surface temperature (SST) retrieval algorithm up to 0.3 K in the global daily-averaged products which causes an apparent spike in the SST time series. Our investigation reveals that this bias is caused by a fundamental but flawed theoretical assumption in the VIIRS calibration equation, which states that the shape of the calibration curve is assumed unchanged from prelaunch to postlaunch without any constrains. While the assumption may work to account for long-term degradation, it has a shortcoming during the blackbody unsteady state. In this study, we present a diagnostic and correction method with a compensatory term (L_{trace}) to reconcile the assumption such that it removes the calibration bias during the blackbody temperature changes. The methodology has been tested using historical data, and the results are very positive. The implementation has minimal impacts on the operational data processing system and is readily available for use in operations.

Plain Language Summary This paper studies an anomaly with the VIIRS instrument in the infrared channels which affects sea surface temperature retrievals. It diagnoses the traceability of the calibration and provides a correction to resolve the issue to improve the quality of the data for all users.

1. Introduction

The long-wave infrared radiometric channels (aka long-wave Thermal Emissive Bands or TEB) of the Suomi National Polar-orbiting Parternership (NPP) Visible Infrared Imaging Radiometer Suite (VIIRS) are primarily used for retrieving sea surface temperature (SST) using the split window algorithm [*Dash et al.*, 2010; *Ignatov et al.*, 2015]. Since the VIIRS TEB data became available on 20 January 2012, the VIIRS TEB calibration has gone through several stages and reached validated maturity on 18 March 2014 [*Cao et al.*, 2014]. Studies have shown that the calibration accuracy is overall excellent with an estimated uncertainty about 0.1 K, based on comparisons with other satellite radiometers such as Moderate Resolution Imaging Spectroradiometer (MODIS), CrIS, and aircraft campaigns [*Cao et al.*, 2013]. The instrument noise in the long-wave TEB is on the order of 0.05 K at 292.5 K, and there is no appreciable change in the instrument responsivity in the long-wave radiometric bands (aka the M bands), which is the focus of this study. One remaining issue is the small but persistent calibration bias found in SST retrievals during the quarterly blackbody temperature warm-up/cooldown (WUCD) operations (aka VIIRS Recommended Operational Procedure (VROP701)). The VIIRS-retrieved SST bias relative to independent models is up to 0.3 K although the bias for single M bands such as M15 is on the order of 0.1 K (https://www.star.nesdis.noaa.gov/sod/sst/micros/#, under "time series").

The relationship between SST and M15 brightness temperature is well documented in the SST algorithm theoretical basis and other publications [*Dash et al.*, 2010; *Ignatov et al.*, 2015] in which this error propagation can be readily analyzed using the SST day time retrieval equations. Our analysis shows that the SST bias indeed was originated primarily from the M15 calibration bias during the WUCD. It is very likely that a calibration bias on the order of 0.1 K will also affect other products using the VIIRS long-wave channels.

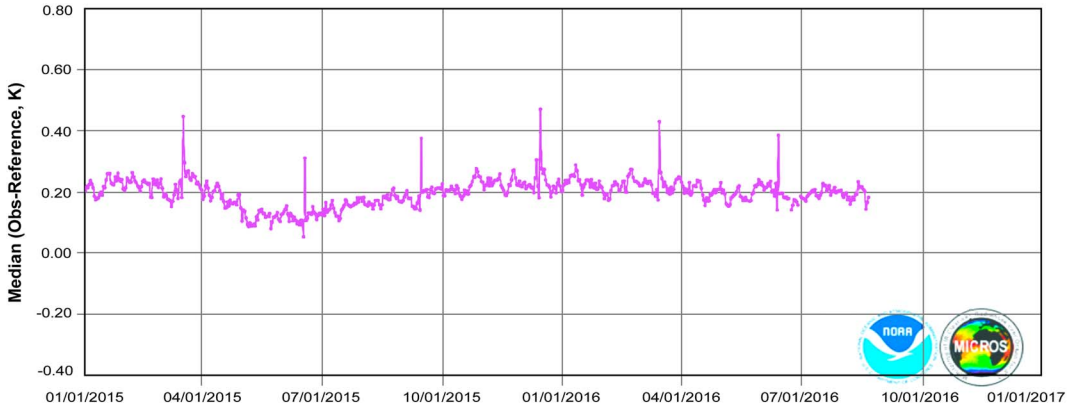

Figure 1. SST anomaly shown as upward spikes in the time series during quarterly WUCD (Source: https://www.star.nesdis.noaa.gov/sod/sst/micros/#).

However, detecting such effects due to small biases is rather challenging in other products because in the case of SST, this bias can only be observed in global daily-averaged brightness temperature long-term time series. For other products such as land surface temperature and emissivity retrievals [*Li et al*., 2010, 2011], the effect should be expected and can be evaluated analytically although may not be easily noticeable in the products.

Detailed analysis of the anomaly shows that this bias is dominated by a positive bias during the 24 h blackbody temperature cooldown phase, although the negative bias during the warm-up phase is less noticeable due to the smaller magnitude and shorter duration. Separately, there is also a known cold bias on the order of 0.3 K when VIIRS M15 observes cold scenes (at or below 200 K) based on comparisons with CrIS. However, this cold scene bias has no direct effect on SST and is not directly related to the WUCD bias and therefore is out of the scope of the current study. There is also a constant cold bias on the order of 0.1 K relative to CrIS at all times which may not be directly related to the WUCD bias as discussed later. To put this bias magnitude in perspective, observed brightness temperature varies greatly from one pixel to the next on the order of several degrees. As a result, a 0.1 K bias is extremely difficult to assess unless with a great deal of averaging both globally and temporally.

Figure 1 shows typical examples of the SST bias in the time series in which each data point represent the SST global daily-averaged differences between VIIRS-retrieved SST and reference models during day time. The upward spikes are the VIIRS M15 observation biases which occur during the quarterly WUCD operations on the second day which is the cooling period.

Further zoom in on each WUCD event reveals that during such events, one of the calibration coefficients (called the *F* factor as discussed in detail later) has an anomalous behavior that is closely related to the blackbody temperature. Figure 2 shows that during the blackbody warm-up, the *F* factor for M15 decreases and vice versa during the blackbody cooldown. The warm-up period is shorter (15 h) than the cooldown period (24 h), and the magnitude of the change for the latter is also larger than during warm-up. As discussed later, since the *F* factor acts as a multiplier to the calibrated radiances, any erroneous fluctuations in the *F* factor will directly introduce bias in the Earth-observed radiances. To perform a thorough investigation, the calibration algorithm is dissected in the next section to evaluate the role

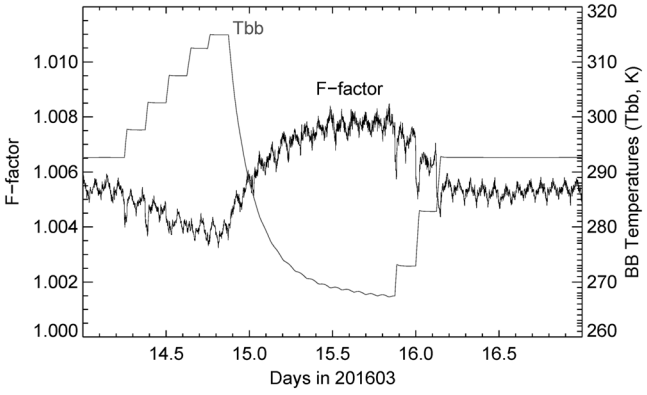

Figure 2. VIIRS onboard blackbody temperature (Tbb) change during WUCD and correlation with *F* factor for M15 (Sample data from March 2016 WUCD event, detector 1, HAM-A shown here; others similar).

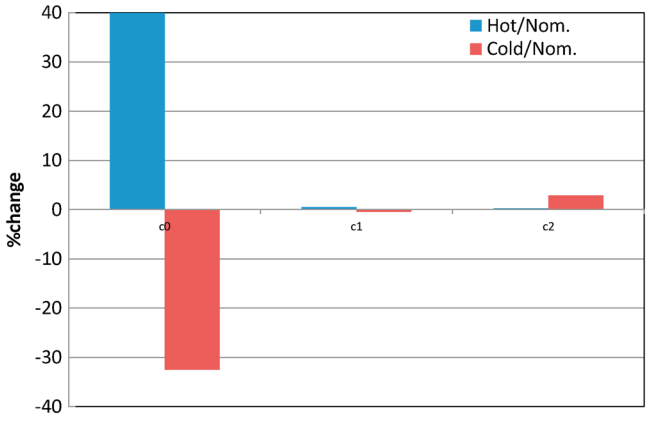

Figure 3. *C* coefficient percent change under different instrument temperature from prelaunch tests (note c_0 change was >80% and off chart).

of *F* factor and its behavior. It should be noted that other infrared channels have similar behavior during the WUCD, although the magnitude of the anomaly becomes smaller toward the shorter wavelength channels (at instrument noise level). The instrument-operating temperature around 292.5 K is near the peak thermal emission for the long-wave channels spectrally. Any temperature change will introduce a larger effect for long-wave infrared calibration. Therefore, this study focuses on the long-wave infrared channels.

2. Calibration Traceability From Prelaunch to Postlaunch According To the VIIRS Radiometric Calibration Algorithm Theoretical Basis

The VIIRS TEB calibration relies on measurements at two calibration points: the onboard calibrator blackbody view (or OBCBB) and views of the deep space (aka space view) on a scan by scan basis. One challenge is to accurately account for the nonlinear response of the instrument. Since the instrument nonlinearity cannot be easily determined after launch, it has to be transferred from prelaunch testing with an external blackbody (known as blackbody calibration source or BCS) in a laboratory environment. Although this is a typical problem for infrared radiometers, the philosophy of transferring prelaunch calibration to on-orbit is very different in the VIIRS radiometric calibration algorithm theoretical basis compared to the heritage approach.

A nonlinear calibration curve is determined by three coefficients: c_0, c_1, and c_2 (Figure 3). Let us call the c_1 the linear slope, c_2 the quadratic term, and c_0 as the offset compensator (discussed later). In the case of heritage methods such as those of MODIS and the Advanced Very High Resolution Radiometer, the linear slope is dynamically calculated and applied on-orbit based on measurements with the onboard blackbody, while the quadratic term is carried over from prelaunch tests and is static unless it is updated as needed [*Xiong and Chang*, 2009; *Datla et al*., 2016].

In contrast to the MODIS and heritage algorithms, the VIIRS algorithm takes a very different approach by carrying all three terms from prelaunch to on-orbit. In other words, the philosophy is that the prelaunch laboratory test using the National Institute of Standard and Technology (NIST) traceable large area blackbody calibration source (BCS) provides the best characterization of the instrument and the derived coefficients from prelaunch are the most reliable. All postlaunch calibration could be made traceable to prelaunch measurements. Therefore, the prelaunch BCS test provides the radiometric reference standard, from which the following calibration equation is established

$$L_{\text{model}} = c_0 + c_1 \cdot dn_{\text{bb}} + c_2 \cdot dn_{\text{bb}}^2 \tag{1}$$

where c_0, c_1, and c_2 are coefficients derived from prelaunch test data. L_{model} is the modeled blackbody radiance based on blackbody temperature measured by the six embedded thermistors and radiative interaction including blackbody emitted, reflected, and mirror emitted radiances, as well as response versus scan angle (RVS) effects

$$L_{\text{model}} = \text{RVS}_{\text{bb}}(\varepsilon_{\text{bb}} L_{\text{bb}} + (1 - \varepsilon_{\text{bb}}) \cdot L_{\text{env}}) + (\text{RVS}_{\text{bb}} - \text{RVS}_{\text{sv}}) \cdot L_{\text{mirror}} \tag{2}$$

where RVS_{bb} is the response versus scan angle factor when viewing the blackbody (relative to the RVS_{sv} of space view which is set to 1); L_{bb} is the computed band-averaged blackbody radiance based on blackbody thermistor measurements; L_{env} is the environmental radiance incident on the blackbody; and L_{mirror} is the mirror emission due to differences in the response versus scan angle, dominated by the half angle mirror (HAM), and the rotating telescope assembly. Equation (2) is a simplified version of the equation 37 in

Datla et al., 2016, in which the terms are ordered in significance of contribution following the traditional infrared calibration equation. The full equation with all detailed terms can be found in the *Joint Polar Satellite System (JPSS) VIIRS Sensor Data Records (SDR) Algorithm Theoretical Basis Document (ATBD)* (*VIIRS ATBD*) [2013].

If the instrument response remains identical from prelaunch to postlaunch, the on-orbit calibration could simply use the same equation (1) and calibration coefficients as those from prelaunch. However, it is known that an instrument will likely degrade over time, and the instrument response may also change due to differences in operating conditions, so the calibration on-orbit needs to be updated. On the other hand, there are three calibration coefficients in equation (1) (c_0, c_1, and c_2), while there is only one blackbody at a nominal temperature which leads to one known parameter with two unknowns in on-orbit calibration. This is a major dilemma in transferring prelaunch nonlinear calibration to on-orbit.

According to the *VIIRS ATBD* [2013], it was decided that an assumption had to be made to make this calibration transfer from prelaunch to on-orbit possible. It was assumed that the degradation can simply be represented by a single *F* factor.

$$F = \frac{L\text{model}}{c_0 + c_1 \cdot dn\text{bb} + c_2 \cdot dn\text{bb}^2} \tag{3}$$

Apparently, for prelaunch test data, *F* factor is unity based on equation (1). With the *F* factor, the degradation of the instrument can be accounted for using the following equation with prelaunch coefficients (c_0, c_1, and c_2) for calculating Earth view radiances (L_{ev}):

$$L_{ev} = \frac{F\left(c_0 + c_1 \cdot dn + c_2 \cdot dn^2\right) - \left(RVS_{ev} - RVS_{sv}\right) \cdot L_{mirror}}{RVS_{ev}} \tag{4}$$

The key assumption made here is clearly stated in the *VIIRS ATBD* [2013] document (page 84).

> "Equation (3) is used on-orbit to update the coefficients. However, since there are three unknowns in one equation, some assumptions or constraints need to be made in order to solve for the coefficients. Making the assumption that the **shape of the response curve is preserved** allows the application of same scale factor F to all three coefficients. The updated coefficients, designated as C_0 to C_2, are scaled equally by the change in scale (or gain) of the response".

This indeed is a convenient solution based on a simple assumption. Simply stated, the VIIRS on-orbit TEB calibration uses prelaunch calibration coefficients, except that it is scaled using the scalar *F* factor to account for any changes from prelaunch to postlaunch, and these changes in the three calibration coefficients are assumed always proportional. But can this critical assumption of calibration curve shape "preserved" hold true under all conditions? Analysis shows that there are several issues with the above quoted statements. First of all, it is not clear what the physics behind the assumption is for this shape of the response curve is preserved, since it did not provide any reference. It seems that this is just an idea so it would make the calibration conveniently transferred from prelaunch to postlaunch (we assume that this could be true for instrument long-term degradation where the dominant change would be in the c_1); second, assuming this assumption is valid; one could infer that this assumption may be applicable to other infrared radiometers. However, it is known that few other infrared radiometers are using this approach for calibration. For example, MODIS calibration does not rely on this assumption and approach as discussed earlier [*Xiong and Chang*, 2009; *Datla et al*., 2016]. Alternatively, this also raises the question whether other radiometers can use the VIIRS approach to improve calibration performance, which is currently under a separate study; third, if this assumption only works for VIIRS (not other instruments), why does VIIRS has a fundamental physics that is different from other radiometers?

Unfortunately, no explanation is given or can be found as to why the assumption, which is the crux of the problem, is always valid. The physics for its validity is not discussed. So far, we have not been able to find any reference materials (either published or white papers) to support this assumption. As a result, the described assumption above does not give us much confidence because it appears that this is an

irresolvable issue so an unproven assumption like this has to be made to make the algorithm work. Is this assumption valid? In other words, can one assume that the shape of the calibration curve remains the same from prelaunch to postlaunch? In the next section we will examine this issue in detail.

Further analysis reveals that this calibration curve shape issue can be further divided into two separate issues: one is whether the calibration curve shape changes from prelaunch to postlaunch under identical operating condition or configurations; the other is whether the operating conditions or configurations are really the same between prelaunch and postlaunch. The former is far more difficult to prove than the latter, because identical operating conditions do not exist on-orbit matching the prelaunch test. But unfortunately, a discrepancy in either one could defeat the purpose of the *F* factor approach. Here a quick review of the calibration traceability of satellite infrared radiometers will help in understanding the issue.

Calibration traceability for infrared radiometers has a well-established procedure in the NOAA heritage satellite program [*Sullivan*, 1999]. In prelaunch thermal vacuum, the infrared radiometer is typically tested by viewing a high-quality external large aperture blackbody (or blackbody calibration source—BCS for VIIRS) that is traceable to national standards (aka NIST traceable). The BCS is set to different and stabilized temperatures covering the dynamic range of Earth observations to derive the instrument nonlinear response under various conditions. The instrument itself is also set to different and stabilized temperatures (aka plateau temperature) to repeat the BCS test, during which the instrument response to the onboard calibrator blackbody (or OBCBB for VIIRS) at the instrument temperature is also measured.

Several differences are observed comparing the VIIRS prelaunch tests from that of the heritage program: first, the instrument temperature in the case of VIIRS was only tested at three plateau temperatures (hot, nominal, and cold), while in the heritage program it had five instrument plateaus temperatures [*Sullivan*, 1999]. Second, the VIIRS test included WUCD tests prelaunch which are highly relevant to the issues discussed in this study as examined later. Third, for VIIRS, all prelaunch-derived calibration coefficients are used for postlaunch calibration in the operations as it is shown in the *F* factor equation (3), while in the heritage program, only the quadratic term is carried to the on-orbit calibration.

The calibration traceability from on-orbit OBCBB to prelaunch BCS critically relies on the level of agreement between the OBCBB and BCS tests in prelaunch test and analysis. At the same BCS and OBCBB temperatures, the radiances falling on the VIIRS detector in prelaunch thermal vacuum chamber viewing an external blackbody (or BCS for VIIRS) are not identical to that viewing an onboard calibrator blackbody (or OBCBB for VIIRS). There are uncertainties in the prelaunch agreement between OBCBB and BCS due to a number of factors, including the fact that during WUCD viewing the OBCBB, it may not have identical operating conditions or configurations as that of prelaunch thermal vacuum viewing the BCS. It is questionable whether the prelaunch BCS test truly captured the instrument response to the OBCBB on-orbit within the 0.1 K level, which is the subject of the anomaly investigated in this study.

3. Uncertainties in the Assumption of Calibration Curve Shape Found in Prelaunch and Postlaunch Data

If we take this critical assumption of an unchanging calibration curve shape discussed in the previous section at its face value, ignoring its underlining physics for a moment, questions still remain as to under what conditions this assumption is valid. Given the lack of supporting evidence for this assumption, here we analyzed two separate sources of data sets to see whether this assumption can hold true at all times. One data source is the prelaunch test data sets when the instrument was tested under different operating conditions in thermal vacuum chamber. The BCS test results are contained in the so-called VIIRS delta C look-up tables (LUT). There is also the prelaunch WUCD test for consistency check between BCS and OBCBB; the second test data set is the independently derived calibration coefficients on-orbit during the WUCD.

For a nonlinear calibration curve with coefficients c_0, c_1, and c_2 described in equations (1)–(4), according to the VIIRS ATBD, it is argued that any change from prelaunch to postlaunch can be characterized by a single *F* factor, if and only if the on-orbit calibration curve defined by the three *C* coefficients change proportionally. In mathematical terms, this means that

$$f0 = \frac{c_0'}{c_0}; f1 = \frac{c_1'}{c_1}; f2 = \frac{c_2'}{c_2} \tag{5}$$

Table 1. VIIRS M15 Prelaunch Test Calibration Coefficients (From Delta C LUT, Detector 1 Shown Here)

Instrument Plateau Temperature	c_0	c_1	c_2
Hot	−0.010879817	0.006295975	1.4118E−08
Nominal	−0.005951365	0.006266075	1.40866E−08
Cold	−0.004017632	0.006241006	1.44915E−08
Hot to nominal ratio (f_0, f_1, and f_2)	1.828121236	1.004771675	1.002227287
Nominal to cold ratio (f_0, f_1, and f_2)	0.675077333	0.995999248	1.028741478

where c_0', c_1', and c_2' are the coefficients for the on-orbit calibration curve; c_0, c_1, and c_2 are the coefficients for the prelaunch calibration curve.

In other words, the *F* factor is valid if and only if the following is true:

$$f0 = f1 = f2 = F_{\text{factor}} \tag{6}$$

The conditions for equation (6) could be tested using prelaunch and postlaunch test data. It is known that similar WUCD tests were performed prelaunch in thermal vacuum chamber at both instrument and spacecraft level, and ideally, the *C* coefficients derived from prelaunch WUCD should match those derived from the BCS test. The prelaunch and postlaunch WUCD-derived coefficients should also match. This would have been the most relevant comparisons in addressing this discrepancy. Unfortunately, the prelaunch test results show that the uncertainties leading to the disagreements for the coefficients derived from the BCS and OBCBB prelaunch can be larger than 0.1 K, and they may not be consistent from one test to another according to internal reports by the NPP Instrument Calibration Support Team (NICST) [*NICST*, 2011a, 2011b]. In other words, the calibration curve shapes derived from BCS and OBCBB during prelaunch WUCD did not agree. This indeed is likely the root cause for the mismatch in calibration curve shape between prelaunch BCS and the postlaunch WUCD, although a more rigorous analysis would be needed to investigate this difference which are practically beyond the instrument specification from the vendor perspective. It is hopeful that for the next VIIRS on JPSS 1, the prelaunch WUCD test data can be scrutinized and the coefficients compared to postlaunch in the near future once the satellite is in-orbit.

Another analysis that can be performed on the prelaunch test results resides in the delta C LUTs. The idea is to see whether and how the calibration curve shape changes under different instrument-operating conditions (primarily due to component temperature variations). It is understood that this does not answer the question whether the calibration curve shape changed from prelaunch to postlaunch, but it does provide insight on the nature of the calibration curve shape variations. In prelaunch, the VIIRS instrument has been tested in thermal vacuum chamber under various conditions including testing at three instrument plateau temperatures (hot, cold, and nominal) and ramping through a large range of external blackbody (or BCS) temperatures (from 180 to 350 K). Each setting was stabilized before the test data were collected. Here we extracted the VIIRS M15 *C* coefficients (c_0, c_1, and c_2) from the prelaunch test data at different instrument plateau temperatures. The ratios between the *C* coefficients are computed to see whether these ratios are constant across the *C* coefficients as shown in Table 1.

From Table 1, it can be seen that the calibration coefficients did not change in proportion when the instrument component temperature changed. For example, when the instrument plateau temperature changed, the c_0 coefficients changed at least 67–82%, and the c_1 coefficients changed 0.47–0.40%, while the c_2 coefficients changed 0.2–2.8%.

Figure 3 shows graphically that the difference in the change is very large among the three coefficients. While c_0 has the largest change, c_1 has a negative change, and c_2 has a moderate change. Figure 4 shows all values in the delta C LUT which were based on prelaunch tests. It shows the VIIRS M15 channel calibration coefficients under different optics and electronics temperatures. In the operational processing, the actual *C* coefficients used are interpolated based on the component temperatures on-orbit at the time. Figure 4 shows that the *C* coefficients do not change in proportion under most circumstances. In other words, this shows that the calibration curve shape will not be the same as the operating environment changes. Again, it is understood that this analysis does not answer the question whether the calibration curve shape changes from prelaunch to postlaunch under identical operating conditions, but it does raises concerns and uncertainties about the assumption of calibration curve shape because apparently, the calibration curve can change easily along

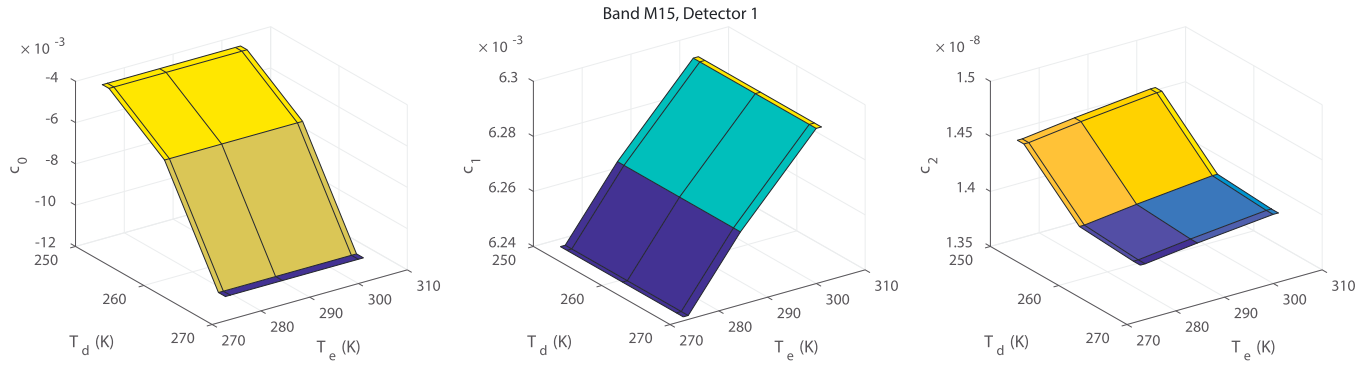

Figure 4. Three-dimensional display of *C* coefficient changes under all conditions (prelaunch test for M15, detector 1, HAM-A; T_d = optomechanical module temperature; T_e = electronics module temperature).

with the operating conditions. Since the instrument-operating conditions are not identical between the prelaunch thermal vacuum chamber and the postlaunch WUCD, it becomes questionable whether the calibration curves derived will match between prelaunch and postlaunch.

Now let us examine the calibration curve shape assumption using on-orbit test data. Is it possible that on-orbit data support the assumption of proportional change in the *C* coefficients or the shape of the response curve is preserved after launch? This is a difficult question to answer because there is no easy way to accurately test the *C* coefficients especially the nonlinear term on-orbit. Since the MODIS era, a periodic blackbody warm-up/cooldown (WUCD) has been developed by NASA MODIS team as a methodology to check the calibration coefficients. The WUCD typically takes 2–3 days during which the blackbody temperature is raised to 315 K step by step by turning on the heater, and then the heater is turned off to let the blackbody temperature drop to its lowest temperature (around 267 K). The idea is that the measurements of radiometer response at different blackbody temperatures may allow us to quantify the nonlinearity of the radiometer response on-orbit.

In this study, the on-orbit calibration coefficients for VIIRS M15 derived from WUCD are compared with those from prelaunch. In deriving the coefficients from WUCD, we separated three data sets in performing the polynomial fitting between L_{model} and *dn* in equation (1): the cooldown data set only, the warm-up data set only, and the combination of both cooldown and warm-up (similar analysis to *Efremova et al*. [2014]). The transient data sets between temperature plateaus which consist of a relatively small sample between stages of warm-up were excluded in the analysis due to anomalous values related to dark current (DC) restore reset. Table 2 shows the WUCD-derived *C* coefficients and their ratios to their corresponding prelaunch *C* coefficients derived from the delta C LUT matching (supposedly) the operating conditions during the WUCD. This is done by extracting the actual *C* coefficients used in the processing of the VIIRS SDR (Sensor Data Record) data. Since the data are extracted from the delta C LUT during the processing of the WUCD data, the *C* coefficients extracted follow the calibration algorithm in retrieving the values based on the configuration and settings for each scan line during the WUCD, although the values presented in Table 2 are granule averages (for M15 detector 1; others similar) due to the limited space here.

The results in Table 2 show that the ratios between WUCD and prelaunch C coefficients have very different values. The f_0, f_1, and f_2 values are not the same (differences of −326%, 0.42%, and −12%), respectively. This means that the two calibration curves have very different shapes, which again violated the assumption for equations (3), (4), and (6) during the WUCD periods which is the focus of this study.

Table 2. Comparison of *C* Coefficients Between Prelaunch and WUCD-Derived Values (WUCD *C* Coefficients From March 2016 Event During Cooldown With Granule Average; M15 Detector 1 Values Shown Here; Others Similar)

	c_0	c_1	c_2
Prelaunch (retrieved from delta C LUT)	−0.005948	0.006273	1.41E−08
Derived from WUCD	0.01360	0.006299	1.24E−08
Percent change (f_0, f_1, and f_2 from WUCD/prelaunch)	−328%	0.42%	−12%

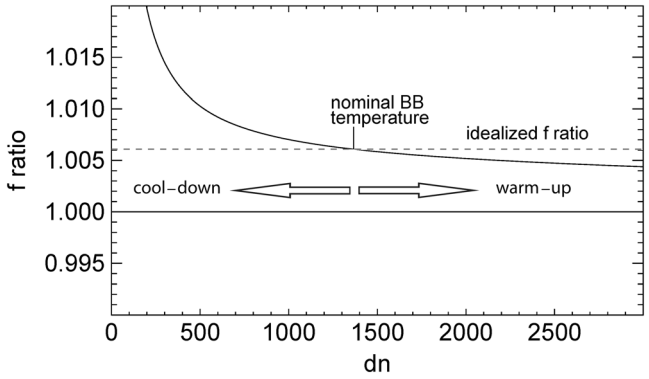

Figure 5. The *f* ratio change as a function of *dn* during WUCD (simulating effects on *f*).

As discussed earlier, the fact that the calibration coefficients from prelaunch WUCD deviated from those from the BCS prelaunch already showed differences in the calibration curve shape between the two. Naturally, the on-orbit-derived calibration coefficients from WUCD cannot be expected to match those from the prelaunch BCS tests.

The discussion above focused on the fact that the calibration curve shapes did not match between postlaunch and prelaunch primarily because the operating conditions are likely different. Now let us examine the issue whether the shape of the response curve really changed from prelaunch to postlaunch under identical conditions which is very difficult to prove. Nevertheless, the assumption of shape of the response curve is preserved from prelaunch to postlaunch is not a commonly accepted concept in radiometric calibration. It is generally understood that the radiometer response changes for a number of reasons. While some of the changes are predictable to a certain extent, such as the degradation leading to lower responsivity, the shape of the curve may not be assumed unchanged under all conditions. This assumption is especially difficult to accept for the c_0 term, which is a fudge factor because the radiance at space view should be zero for the infrared channels, while the equation suggests that the space view radiance is c_0 (nonzero or even negative). The concept of c_0 changing at the same rate as that of the instrument response would be difficult to explain.

In short, the assumption of shape of the response curve is preserved from prelaunch to postlaunch is likely flawed because it may not be true under all conditions. Neither prelaunch test data nor postlaunch WUCD data support this assumption. We believe that the root cause for the calibration biases during WUCD is that the postlaunch calibration curve shape derived from WUCD is different from that of prelaunch, for reasons discussed above.

What happens if the postlaunch calibration curve shape does not match that of the prelaunch? In this scenario the impact on calibration bias is analyzed in this section. When the blackbody temperature on-orbit (OBCBB) is maintained within a very narrow range of 292.5 K ± 0.1 K at all times, the discrepancy in the shape of the response curve is preserved assumption has little effect on the calibration, till the blackbody temperature deviates from the nominal temperature, when the temperature bias begins to increase (Figure 5). This is further analyzed as follows.

The prelaunch and WUCD-derived calibration curves can be compared at different blackbody temperatures by using the following ratio between them

$$f = \frac{c'_0 + c'_1 \cdot dn_{bb} + c'_2 \cdot dn_{bb}^2}{c_0 + c_1 \cdot dn_{bb} + c_2 \cdot dn_{bb}^2} \tag{7}$$

where c_0', c_1', and c_2' again are the postlaunch coefficients derived from WUCD and c_0, c_1, and c_2 values are derived from prelaunch delta C LUT during the WUCD event (all values are presented in Table 2). Using this equation, we input the *dn* (blackbody view count minus space view count) values representing different blackbody temperatures (such as from 270 to 315 K). If the two curves have the same shape, then the *f* ratio would be a constant with respect to different *dn* values. As Figure 5 shows, this is not the case. It shows that during cooldown, the *f* ratio increases, while it decreases during warm-up. Since the *f* directly affects the Earth view radiance calculations as shown in equation (4), this explains why there is positive bias during blackbody cooldown and a negative bias during blackbody warm-up.

While Figure 5 simulates the *f* ratio between on-orbit and prelaunch calibration curves using coefficients from Table 2, Figure 6 shows the actual *F* factor data from the VIIRS SDR product during the WUCD event from

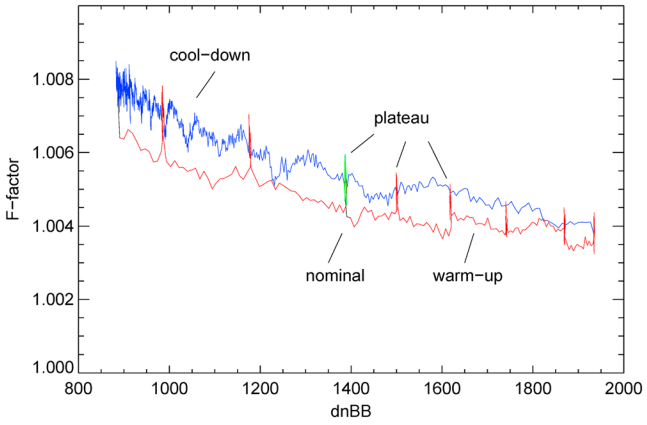

Figure 6. *F* factor change as a function of *dn* (proxy for blackbody temperature; M15 detector 1 shown here; others similar).

March 2016 as a function of instrument output counts or *dn*. There are several observations from this figure: first, generally, there is an inverse correlation between *F* factor values and the *dn*. This means that at colder blackbody temperatures, the *F* factor value is higher by as much as 0.8%, and at warmer blackbody temperature, the *F* factor value is lower by as much as 0.4%. This directly affects the calibrated Earth view radiance as discussed earlier; second, the nominal *F* factor during normal operations with a blackbody temperature of 292.5 K is at 1.05 when the *dn* is at ~1400, compared to 1.0 prelaunch, which suggests that there is a change about 5% from prelaunch to postlaunch; third, during the plateau periods (vertical lines on the chart), the response is in general agreement with the response during cooldown (blue curve converges); finally, there is a difference in the response between warm-up versus cooldown and plateau periods (or the transition period), although the time period for this is relatively short. This is due to the very unsteady state of the blackbody as well as the DC restore mechanism, and therefore, the data during this period are excluded in the analysis (Table 3).

Based on the response curve shape assumption discussed earlier, the *F* factor was originally designed to track the degradation of the instrument based on the assumption that the shape of the curve remains the same from prelaunch to postlaunch. Unfortunately, the pattern shown in Figure 6 is contradictory to the assumption because it suggests that the *F* factor is changing short term (not due to degradation) when the blackbody temperature is changing (inversely correlated). The original assumption was based on the hope that the *F* factor should have been remaining unchanged under all circumstances (presumably including during the blackbody temperature changes), which means that in Figure 6 the curve should have been a flat line. Given the equation of Earth radiance calculation (equation (4)), a positively biased *F* factor by 0.003 would lead to a positive bias by 0.3% in radiance, which exactly matches the M15 bias of ~0.1 K at SST temperature range.

In short, we believe that the root cause of the long-wave infrared channel bias in VIIRS is due to the fundamental assumption of shape of the response curve is preserved from prelaunch to postlaunch which is not supported by the test data during the WUCD period. Even if the shape was actually preserved (which is difficult to prove), it certainly did not match the response curve derived from on-orbit WUCD. When the shapes do not match between prelaunch and on-orbit (in the event of WUCD), an unexpected change in the *F* factor is the result which directly introduces the bias in the long-wave infrared bands.

4. Diagnosing and Reconciling the Assumption of Calibration Curve Shape

Since the root cause of the calibration bias is due to a flaw in the assumption of the calibration curve shape, solutions need to be developed to reconcile this issue. Given the fact that the entire VIIRS calibration algorithm hinges on the calibration curve shape assumption and the algorithm works as expected long-term with respect to instrument degradation, it may not be necessary to make fundamental changes which could have major impacts to the ground processing system. Since this problem only affects the data during a 3 day period of WUCD quarterly, the impact can be mitigated. A reconciliation of the assumption is probably an

Table 3. Example Component Temperatures During WUCD

	OBCBB at 292.5 K	OBCBB at 270 K	OBCBB at 320 K
Half angle mirror(HAM)	265.42	265.35	266.07
Instrument (or OMM)	262.86	262.52	263.83
Electronics	284.84	284.73	285.05

efficient approach in solving this problem during WUCD. Nevertheless, there are several options to reconcile the issue, and we encourage future studies to investigate them, as well as other solutions:

1. Ideally, the same WUCD procedure with identical configuration both prelaunch and postlaunch needs to be performed and data rigorously analyzed to resolve any inconsistencies between them, as well as with the BCS prelaunch test, which is the underpinning for on-orbit radiometric traceability. The current practice of testing and analyzing the agreement between BCS and WUCD data prelaunch has uncertainties greater than 0.1 K level which cannot resolve the inconsistency between BCS and WUCD data either prelaunch or postlaunch as discussed earlier. This uncertainty raises questions whether the calibration curves derived from WUCD postlaunch will ever match that of the prelaunch BCS test because the curves are derived at different conditions from different blackbodies. On the other hand, practically, since this WUCD issue was not discovered till after launch, it is difficult to foster additional testing and analysis at this stage, although this should be a recommended enhancement for future prelaunch testing and analysis.
2. Use calibration coefficients derived from WUCD on-orbit for operational calibration. The current algorithm uses the prelaunch-derived calibration coefficients which cannot be reconciled with those from WUCD either postlaunch or prelaunch. One solution is to use WUCD-derived coefficients or incorporate them in the delta C LUT for the operational calibration, which should resolve the inconsistency. Our recent tests using this approach show that it can successfully remove the bias during WUCD, and in fact it works well for all TEB bands. In this case there will be no discrepancy between response curve shapes to speak of because there is only one curve used. However, there are drawbacks with this approach. For example, this may cause a sudden change in the operational production of VIIRS SDR data which will affect time series analysis unless reprocessing of all data is performed. The temperature-dependent calibration coefficients captured in the delta C LUT may be lost which may affect the calibration accuracy under different conditions. This also implies that the traceability from postlaunch to prelaunch may not be well established as originally designed, which is not consistent with what was planned in the VIIRS ATBD. Finally, the efficiency of forcing more than 90% of the data during normal operations to match those during the WUCD requires further assessment, especially when the absolute accuracy of using on-orbit WUCD data for calibration has not been established. Further studies are needed using this approach, and its suitability for a new satellite such as JPSS 1 would be more beneficial for a consistent time series in the future.
3. Adjust the radiometric model parameters in L_{model} in equation (2) to make it fit to the WUCD data. This can be done only if we believe the following assumptions: (a) the differences in the instrument-operating conditions between prelaunch test in thermal vacuum chamber against the BCS versus WUCD with OBCBB can be addressed; (b) the calibration curve shape really must be the same between WUCD and prelaunch tests, which has not been proven as discussed earlier. Nevertheless, there are parameters that can be adjusted, including a number of parameters in the L_{model}, such as the L_{mirror}, or RVS (or both) in the numerator of equation (3), assuming that a room for coefficient adjustments exists for prelaunch test data. An iterative approach will have to be used because the prelaunch coefficients (aka delta C LUT) themselves are derived based on the same model. A change in the model parameters will also change the prelaunch coefficients. There is also the offset compensator (aka c_0) which is practically a fudge factor due to the lack of physical foundation for this term. Unfortunately, any changes in the model will likely affect all calibrated data since launch which is nontrivial. Such approach will still be based on the questionable assumption of calibration curve shape preserved, which may not be true under all conditions. Similarly, the delta C LUT can also be adjusted based on WUCD-derived coefficients which can modify the denominator in equation (3). Such adjustments may be justifiable under the assumption of within the uncertainties in the previously derived parameters.
4. Diagnose the calibration bias during the WUCD period by introducing a correction term to the WUCD calibration coefficients to reconcile the curve shape assumption. The idea behind this approach is that although we cannot fully validate or invalidate the calibration shape curve assumption, the current algorithm works well enough in producing a consistent SST product during normal operations. Therefore, what is needed is to perform a localized correction only during the WUCD period. By introducing a compensatory term called L_{trace}, the calibration curve shapes between WUCD and prelaunch can be made match, and therefore, the bias anomaly can be removed. In this paper, we explore this approach in detail next.

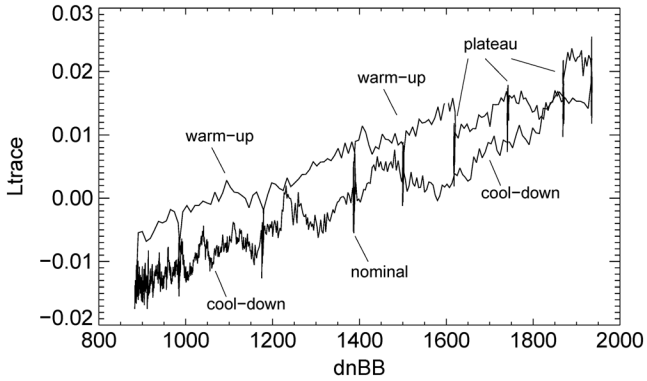

Figure 7. Example L_{trace} and its correlation with blackbody *dn* for VIIRS M15 during WUCD (detector 1 shown here; others similar).

Given the fact that both the SST and the OBCBB are normally stable short term based on global daily average values, the VIIRS calibration anomaly can be diagnosed and reconciled by introducing a compensatory term called L_{trace}, such that the calibration curve during WUCD matches the shape of the prelaunch calibration curve. This makes the WUCD calibration curve proportional to the prelaunch curve, which satisfies the curve shape assumption. Mathematically, based on equation (3), this means that

$$\begin{aligned} F &= \frac{\mathrm{RVS_{bb}}[\varepsilon_{bb}L_{bb} + (1-\varepsilon_{bb})\cdot L_{env}] + (\mathrm{RVS_{bb}} - \mathrm{RVS_{sv}})\cdot L_{mirror} + L_{trace}}{c_0 + c_1\cdot dn_{bb} + c_2\cdot dn_{bb}^{\ 2}} \\ &= f\frac{c_0 + c_1\cdot dn_{bb} + c_2\cdot dn_{bb}^{\ 2} + L_{trace}}{c_0 + c_1\cdot dn_{bb} + c_2\cdot dn_{bb}^{\ 2}} \\ &= \frac{L_{WUCD}}{L_{prelaunch}} \end{aligned} \tag{8}$$

L_{trace} can be solved numerically,

$$L_{trace} = F_{norm}\cdot\left(c_0 + c_1\cdot dn_{bb} + c_2\cdot dn_{bb}^{\ 2}\right) - \mathrm{RVS_{bb}}(\varepsilon_{bb}\cdot L_{bb} + (1-\varepsilon_{bb})\cdot L_{env}) - (\mathrm{RVS_{bb}} - \mathrm{RVS_{sv}})\cdot L_{mirror} \tag{9}$$

L_{trace} is a diagnostic term, and it represents the radiance difference between prelaunch and postlaunch curves and can be derived using WUCD data by applying the ideal short-term nominal constant *f* ratio (or F_{norm}) which is the nominal *F* value at the typical blackbody temperature of 292.5 K at the time before and after the WUCD event.

Figure 7 shows an example of L_{trace} for M15 (detector 1, HAM-A; others similar) during the WUCD event in March 2016 (others have similar pattern). Analysis of WUCD data shows that the L_{trace} has several characteristics here:

1. L_{trace} is near zero at nominal BB temperature, but it becomes a positive value when higher than nominal and negative value when lower than nominal.
2. For the long-wave infrared bands such as M14, M15, and M16, L_{trace} can be modeled as a function of blackbody radiance (or *dn*) and then fed back to the L_{model} to make the *F* factor flat. Our study shows that a simple linear or polynomial fit between blackbody *dn* and L_{trace} works well; alternatively, the *F* factor during nominal operating periods can be used to replace those during WUCD which would make the *F* factor identical to those during normal periods, but that would require the use of a much large correction data set or LUT, compared to the modeling approach.
3. In calculating L_{trace}, the F_{norm} value is taken as the nominal *F* factor value during normal operations immediately before and after a specific WUCD event. The F_{norm} is treated as a constant for a specific WUCD event although it is expected to change from one WUCD event to another as this is the case with the *F* factor changes in the long term.
4. Once the L_{trace} coefficients are derived from one WUCD event, it can be applied to all other WUCD events. This means that the correlation between blackbody temperature and L_{trace} does not change over time despite that the *F* factor (and the F_{norm} for each WUCD event) may change.

As it is shown in Figure 8, L_{trace} can be applied to the calibration as a function of blackbody temperature. After the L_{trace} is applied to the calibration, the *F* factor during the WUCD becomes flat. The remaining oscillations (0.05% or ~30 mK) are dominated by orbital variations that existed previously during normal operations.

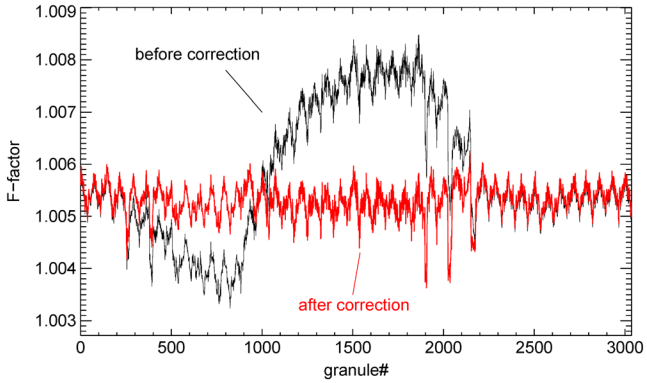

Figure 8. Correction to the *F* factor using the L_{trace} algorithm (M15 detector 1 shown here; others similar).

The L_{trace} method has been successfully tested in the sample reprocessing of VIIRS SDR data. It has been shown that it effectively removed the M15 bias which is the dominant source for the SST biases during WUCD. Figure 9 shows the time series of orbital-averaged nadir observations during the warm-up/cooldown period. It demonstrates that after the correction, the observed brightness temperature was increased during the blackbody warm-up period slightly and decreased about 0.1 K during the cooldown period. Note that the orbital average temperature variation can be more than a degree so this correction is smaller by comparison. Another way to show the effectiveness of the correction is to take the before and after differences in brightness temperature. The difference in brightness temperature as shown in Figure 9 shows clearly the correction worked, and the correction curve closely matched the *F* factor curve presented in Figure 8 as expected.

The biases for other bands are smaller, although for some bands (such as M16 and M13), a nonlinear fit or a much larger LUT may be required for the L_{trace} coefficients for better performance. Extensive validation of the correction has been performed using a number of approaches, including collocated time series before and after comparisons for SST, independent comparisons with CrIS (J. Li and L. Wang, personal communications, 2017), and comparisons with radiative transfer model CRTM (X. Liang, personal communication, 2017). All studies reported that the M15 bias has been successfully removed using the L_{trace} algorithm. Given the limited length and scope of this paper, the implementation and validation of the algorithm and extended validation results are presented in other papers [i.e., *Wang et al*., 2017].

It should be noted that the L_{trace} presented in equation (8), together with equation (7), is a diagnostic method and tool to assess the agreement between prelaunch and postlaunch calibration or the traceability, and it can be used as a localized empirical solution during the WUCD period to a rather complex problem of prelaunch to postlaunch calibration traceability and related uncertainties. Although the L_{trace} method does not restore radiometric traceability from postlaunch to prelaunch, it enables us to assess the traceability quantitatively. For example, when the postlaunch calibration coefficients match those from the prelaunch, the L_{trace} values would be zero, and the *f* values in equation (7) would become a constant, which indeed is the case when on-orbit WUCD-derived coefficients are used in place of the prelaunch coefficients in calculating the *F* factors in equations (2) and (3), as discussed in section 2. A nonzero L_{trace} would suggest discrepancies between prelaunch and postlaunch traceability. The L_{trace} method can be used to diagnose any solutions discussed earlier, and we envision that this tool can be extended to diagnose the traceability of other radiometers as well.

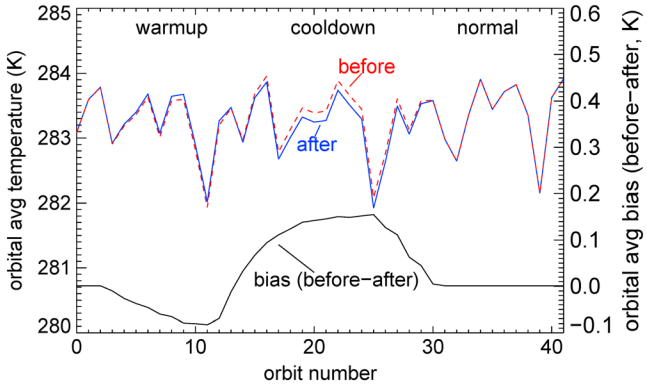

Figure 9. Earth view brightness temperature difference before and after using the L_{trace} algorithm (orbital Earth view average between 275 K and 295 K shown here; orbital average temperature = left axis, bias = right axis).

5. Conclusions

The VIIRS long-wave channel operational calibration relies on the assumption of calibration curve shape being preserved from prelaunch to postlaunch. This assumption is

necessary because there are three *C* coefficients in the calibration equation, while only one can be determined regularly on-orbit with blackbody calibration. The study shows that this assumption has a fundamental flaw because it may not be valid during the blackbody unsteady states based on analysis of prelaunch and postlaunch test data. We demonstrated that the calibration curve differences between prelaunch and on-orbit during WUCD in fact are most likely the culprit for the calibration bias during such events. It is likely that the mismatch in the calibration curve shape arises from different instrument-operating conditions between prelaunch in the thermal vacuum chamber viewing the BCS versus viewing the OBCBB on-orbit during the WUCD period. On the other hand, the assumption has limited effect on the long-term trend of the calibration during normal operations, which is dominated by a slow long-term responsivity changes over time or degradation. Therefore, a diagnostic method with a localized correction algorithm using a compensatory term (L_{trace}) is presented in this study to mitigate the calibration bias during the WUCD period, and the result shows that the bias has been effectively corrected based on independent validations. The VIIRS calibration algorithm, despite this shortcoming, has been working well during normal operations, and the VIIRS data have been used for a large number of global applications. The bias correction presented here further improves the quality of the VIIRS data for the periods of blackbody temperature changes or unsteady states.

Acknowledgments

The authors would like to thank the VIIRS SDR team members for fruitful discussions on the problem and possible solutions discussed in this study. Thanks are extended to Likun Wang, Jun Li, and Xingming Liang, for independent validation of the proposed algorithm and reprocessed results. This study is partially funded by the JPSS program. All data used in this study are publicly available through the NOAA class archive. The manuscript contents are solely the opinions of the author(s) and do not constitute a statement of policy, decision, or position on behalf of NOAA or the U. S. Government.

References

Cao, C., J. Xiong, S. Blonski, Q. Liu, S. Uprety, X. Shao, Y. Bai, and F. Weng (2013), Suomi NPP VIIRS sensor data record verification, validation, and long-term performance monitoring, *J. Geophys. Res. Atmos.*, *118*, 11,664–11,678, doi:10.1002/2013JD020418.

Cao, C., F. Deluccia, X. Xiong, R. Wolfe, and F. Weng (2014), Early on-orbit performance of the visible infrared imaging radiometer suite onboard the Suomi National Polar-Orbiting Partnership (S-NPP) Satellite, *IEEE Trans. Geosci. Remote Sens.*, *52*(2), 1142–1156, doi:10.1109/TGRS.2013.2247768.

Dash, P., A. Ignatov, Y. Kihai, and J. Sapper (2010), The SST Quality Monitor (SQUAM), *J. Atmos. Ocean. Technol.*, *27*(11), 1899–1917, doi:10.1175/2010jtecho756.1.

Datla, R., X. Shao, C. Cao, and X. Wu (2016), Comparison of the calibration algorithms and SI traceability of MODIS, VIIRS, GOES, and GOES-R ABI sensors, *Remote Sens.*, *8*(2), 126.

Efremova, B., J. McIntire, D. Moyer, A. Wu, and X. Xiong (2014), S-NPP VIIRS thermal emissive bands on-orbit calibration and performance, *J. Geophys. Res. Atmos.*, *119*, 10,859–10,875, doi:10.1002/2014JD022078.

Ignatov, A., B. Petrenko, Y. Kihai, J. Stroup, P. Dash, X. Liang, I. Gladkova, X. Zhou, J. Sapper, and F. Xu (2015), *JPSS SST Products at NOAA in EUMETSAT 2015*, edited, p. 9, Toulouse, France. [Available at (ftp://ftp.star.nesdis.noaa.gov/pub/sod/osb/aignatov/EUMETSAT/2015_09_25_EUMETSAT_VIIRS_Ignatov_v04.pptx).]

Li, J., Z. Li, X. Jin, T. Schmit, L. Zhou, and M. Goldberg (2011), Land surface emissivity from high temporal resolution geostationary infrared imager radiances: Methodology and simulation studies, *J. Geophys. Res.*, *116*, D01304, doi:10.1029/2010JD014637.

Li, Z., J. Li, X. Jin, T. J. Schmit, E. Borbas, and M. D. Goldberg (2010), An objective methodology for infrared land surface emissivity evaluation, *J. Geophys. Res.*, *115*, D22308, doi:10.1029/2010JD014249.

NICST (2011a), Analysis of the radiometric calibration from VIIRS F1 RC-05 Part 2 Test (nominal plateau), Internal Memo, 11–002.

NICST (2011b), Spacecraft level testing of thermal band radiometric calibration using the on-board blackbody, Internal Memo, 11–006.

Sullivan, J. (1999), New radiance-based method for AVHRR thermal channel nonlinearity corrections, *Int. J. Remote Sens.*, *20*(18), 3493–3501.

Xiong, X., and T. Chang (2009), Performance of MODIS thermal emissive bands on-orbit calibration algorithm, *Geosci. Remote Sens. Symp.*, doi:10.1109/IGARSS.2009.5417754.

VIIRS ATBD (2013), Joint Polar Satellite System (JPSS) Visible Infrared Imaging Radiometer Suite (VIIRS) Sensor Data Records (SDR) Algorithm Theoretical Basis Document (ATBD). [Available at https://ncc.nesdis.noaa.gov/documents/documentation/ATBD-VIIRS-RadiometricCal_20131212.pdf.]

Wang, W., C. Cao, B. Zhang, and L. Wang (2017), Operational correction and validation of the VIIRS TEB longwave infrared band calibration bias during blackbody temperature changes, SPIE Optics and Photonics.